Episodic Synchronization via Dynamic Injection

Javier M. Buldú,[1] Tilmann Heil,[2] Ingo Fischer,[2,*] M. C. Torrent,[1] and Jordi García-Ojalvo[1]

[1]*Departament de Física i Enginyeria Nuclear, Universitat Politècnica de Catalunya, Colom 11, 08222 Terrassa, Spain*

[2]*Institut für Angewandte Physik, Technische Universität Darmstadt, Schloßgartenstraße 7, D-64289 Darmstadt, Germany*

(Received 18 March 2005; published 17 January 2006)

We report the occurrence of spontaneous synchronizing events between two semiconductor lasers, when the emission of a frequency- and intensity-chaotic driving laser is unidirectionally coupled into a second stable response laser. The driving laser is driven chaotic by delayed optical feedback, the response laser is a device-identical solitary laser. We demonstrate the onset of an episodic synchronization regime when the two lasers are spectrally detuned with respect to each other. By a joint experimental and modeling analysis we can attribute the onset and the duration of the episodes to properties of spectral overlap of both lasers. This effect can even give rise to seemingly anticorrelated intensity behavior. We expect episodic synchronization to be a generic scenario for the loss of synchronization of chaotic oscillators exhibiting frequency cycles.

DOI: 10.1103/PhysRevLett.96.024102 PACS numbers: 05.45.Xt, 42.55.Px, 42.65.Sf

Synchronization of complex dynamics arises frequently in coupled systems, either as a by-product of or as a requirement for an underlying information exchange. Examples include interacting physiological systems [1] and coupled lasers [2], among many others (see [3,4] for thorough reviews). Most studies performed so far in model systems have dealt with steady synchronization states. However, complex systems such as the brain rely on *transient episodes* of synchronization [5], sometimes called microstates or quasistationary states [6]. These states are functionally relevant, e.g., in cognitive processes [7], but the complexity of the brain precludes an understanding of their origin. Here we present experimental evidence of the occurrence of sporadic synchronization events in a well controlled and well characterized physical setup, consisting of two unidirectionally coupled semiconductor lasers. This *episodic synchronization* arises in the transition between desynchronized and fully synchronized dynamics, and can be envisioned as a generic ''route to synchronization'' in coupled chaotic oscillators exhibiting frequency chaos.

Semiconductor lasers subject to delayed optical feedback exhibit chaotic dynamics comprising chaotic intensity pulsations on subnanosecond time scales and significantly slower chaotic frequency cycles, on typical time scales of nanoseconds to microseconds. When this dynamical state is injected into a second, solitary laser, the difference between the optical frequencies of the two lasers becomes a relevant parameter [8]. Several investigations have determined the range of detuning values allowing significant intensity correlations in this system [9–13]. However, the question of how the system of coupled semiconductor lasers loses synchronization has not been studied much so far. In this Letter we concentrate on this question.

Typical scenarios for the loss of synchronization that have been reported in coupled oscillator systems are on-off intermittency, bubbling, intermittent lag synchronization, and imperfect phase synchronization [4]. In the particular case of semiconductor lasers, intermittent lag synchronization due to parameter mismatches has been reported numerically [14]. In all those scenarios an otherwise stable synchronized state is interrupted by sudden desynchronizing events. In this Letter we give evidence for a fundamentally different scenario that is characteristic for systems with chaotic frequency cycles: episodic synchronization. In this scenario the systems can be desynchronized most of the time, interrupted by sporadic synchronization episodes. The onset and duration of these episodes can be attributed to the spectral dynamics of the driving laser, and depend on the instantaneous frequency detuning between the driving and the response systems.

We consider a situation in which the driving semiconductor laser is subject to delayed optical feedback and set to operate in the low-frequency-fluctuation (LFF) regime. This regime, which has been well investigated, is characterized by intensity dropouts at irregular times associated with the combined intensity and frequency dynamics mentioned above. The output of the driving laser is injected into a solitary response laser, i.e., a laser without optical feedback. We have selected two device-identical lasers (Hitachi HLP1400 Fabry-Perot semiconductor lasers, adjusted optical spectra agree within 0.1 nm, slope efficiency within 2%, and threshold current within 5%) obtained from the same wafer, in order to have as similar properties as possible. Both lasers have been pumped by a low-noise dc current source, and temperature stabilized to better than 0.01 K. The driving laser has been exposed to moderate optical feedback giving rise to a threshold reduction of 6%. The lasers are coupled unidirectionally via the injection of a well-defined fraction of the optical field of the driving laser into the response laser. The intensity dynamics of both lasers have been detected simultaneously with 6 GHz photodetectors and analyzed using an oscilloscope of 1 GHz analog bandwidth. In our experiments both lasers are driven at their solitary threshold current $I_{\mathrm{th}}^{\mathrm{sol}}$. We have carefully adjusted the detuning between the optical fre-

quencies of the two lasers by slight variations of the temperature of the response laser while keeping all other parameters constant.

Our aim is to study what happens when the spectral overlap between the driving laser and the locking range of the response laser decreases. Consequently, we choose as control parameter the detuning, defined as the difference between the optical frequencies of the free-running driving and response lasers. For zero detuning, both lasers emit at the same frequency and stable synchronization between the output intensities occurs [9]. When a small detuning is introduced, synchronization is affected. The left panel of Fig. 1 shows the typical experimentally measured dynamics of the driving-response lasers for positive [1(a)], zero [1(b)], and negative [1(c)] detuning. We note that the full dynamics, consisting in fast—subnanosecond—intensity pulses [see Fig. 2(e) and Ref. [15]] has been filtered by the finite bandwidth of the oscilloscope. As expected, at zero detuning the response laser reproduces the dynamics of the driving laser [Fig. 1(b)], which manifests itself in high temporal correlation and well-agreeing corresponding rf spectra (not shown). For slightly positive detuning of a few GHz, the quality of the synchronization is gradually lost: the intensity dropouts remain well synchronized, but the total power of the response laser decreases with a positive increase of the detuning and the shape of the response dropouts is slightly modified [Fig. 1(a)]. Remarkably, this behavior is not symmetric with respect to the sign of the detuning: for negative detuning, the intensity of the response laser shows jump-ups instead of dropouts, coinciding with the intensity dropouts of the driving laser [Fig. 1(c)], a behavior that is not observed for positive detuning. As we will see, these intensity jump-ups at negative detuning correspond to episodic synchronization occurring during a frequency cycle after an intensity dropout of the driving laser.

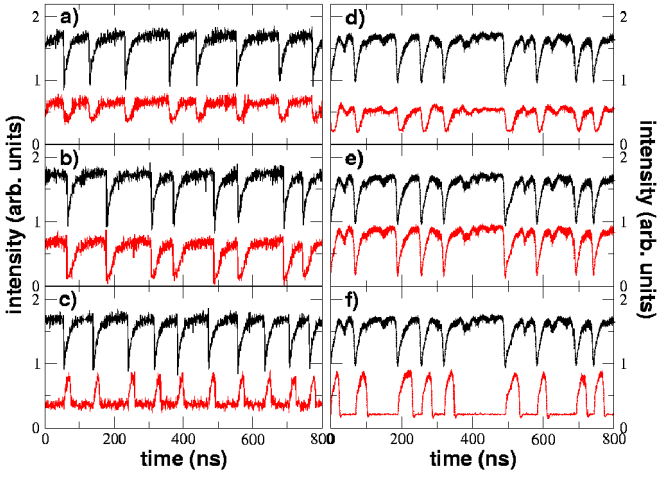

FIG. 1 (color online). Output intensities of the driving (upper trace in each plot) and response (lower trace) lasers for three different frequency detunings. The time traces are separated via a vertical displacement for clarity. Left panel: experimental results with detuning 9 GHz (a), 0 GHz (b) and −10 GHz (c). Right panel: numerical results with detuning $\Delta f = \Omega/2\pi = 15.91$ GHz (d), $\Delta f = 0$ GHz (e), and $\Delta f = -3.987$ GHz (f). The parameters used in the numerical simulations are $C = 1.01$, $\gamma_e = 6.890 \times 10^{-4}$ ps^{-1}, $\gamma = 0.480$ ps^{-1}, $g_N = 1.20 \times 10^{-8}$ ps^{-1}, $\alpha = 4.0$, $N_0 = 1.25 \times 10^8$, $\beta = 10^{-10}$ ps^{-1}, $\kappa_f = 0.030$ ps^{-1}, $\kappa_c = 0.030$ ps^{-1}, $\tau_f = \tau_c = 3$ ns, $\omega_t \tau_f = 0$.

With the aim of gaining insight into the mechanism generating the intensity jump-ups, we have performed numerical simulations of the situation described above. The driving laser is described by the Lang-Kobayashi (LK) model [12], and the response laser by a standard rate-equation model with delayed injection:

$$\frac{dE_t}{dt} = \frac{1 + i\alpha_t}{2}[G_t(|E_t|^2, N_t) - \gamma_t]E_t(t) + \kappa_f e^{-i\omega_t \tau_f} E_t(t - \tau_f) + \sqrt{2\beta N_t}\zeta_t(t), \quad (1)$$

$$\frac{dE_r}{dt} = \frac{1 + i\alpha_r}{2}[G_r(|E_r|^2, N_r) - \gamma_r]E_r(t) + \kappa_c e^{i\Omega t} E_t(t - \tau_c) + \sqrt{2\beta N_r}\zeta_r(t), \quad (2)$$

$$\frac{dN_{t,r}}{dt} = C_{t,r} - \gamma_e N_{t,r} - G_{t,r}(|E_{t,r}|^2, N_{t,r})|E_{t,r}(t)|^2. \quad (3)$$

Here $E(t)$ represents the complex envelope of the electric field and $N(t)$ the carrier number, with the subindices t and r denoting the driving and response lasers, respectively. γ and γ_e are the inverse lifetimes of photons and carriers, α is the linewidth enhancement factor, and $\Omega = \omega_t - \omega_r$ is the detuning between the free-running frequencies of the driving and the response lasers, ω_t and ω_r, respectively. $C_{t,r}$ is the bias current.

The last term in the electric-field Eqs. (1) and (2) represents spontaneous emission fluctuations, with $\zeta_{t,r}(t)$ given by Gaussian white noises of zero mean and unity intensity, and β measuring the internal noise strength. The material-

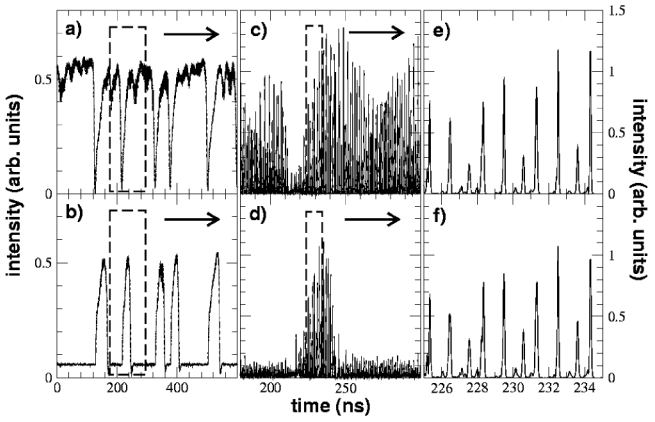

FIG. 2. Numerical time traces of the driving (top) and response (bottom) laser output intensities in the jump-up regime. (a),(b) Correspond to the filtered signal (100 MHz) while (c),(d) and (e),(f) correspond to the unfiltered signals (note the difference in time scales).

gain function is given by $G_{t,r}(|E|^2, N_{t,r}) = g_N[N_{t,r}(t) - N_{0t,r}]$, where g_N is the differential gain coefficient and N_0 is the carrier number in transparency. The optical feedback term of the driving laser is described by the feedback strength κ_f and the external round-trip time τ_f. The optical injection into the response laser [Eq. (2)] depends on the coupling strength κ_c and the delay time τ_c.

In the right panel of Fig. 1 we show numerical results for positive, zero, and negative detuning, which are in qualitative agreement with the experimental observations (left panel). The numerical output intensities have been filtered in order to reproduce the experimental signal measured by a photodetector (to help comparison). Nevertheless, both the driving and the response lasers are emitting fast subnanosecond intensity pulsations. Figure 2 compares their filtered output intensities 2(a) and 2(b) with the unfiltered signals 2(c) and 2(d)—enlargements are shown in 2(e) and 2(f)—for the case of negative detuning. Figures 2(c) and 2(d) reveal that the jump-ups begin with the recovery process of the intensity dropout. In other words, the jump-ups appear *after,* and not during, the intensity dropout of the driving laser. This fact discards an antisynchronization dynamics between the two lasers, like those reported previously in other situations [16]. In fact, it is the synchronization dynamics that induces jump-ups in the response laser. In the enlarged plots of Figs. 2(e) and 2(f) we can observe how during the intensity jump-up there is a high correlation between the fast intensity pulses emitted by the two lasers. This synchronization is suddenly lost after a short transient, thus terminating the jump-up event. We note that the synchronization events are isochronous; i.e., there is no delay between the lasers [12].

We now examine, for the case of negative detuning, (i) why the lasers synchronize right after each intensity dropout of the driving laser, and (ii) why synchronization is suddenly lost during buildup. Two ingredients must be taken into account to solve the problem: first, the mechanism underlying the dynamics of a semiconductor laser in the LFF regime (the driving laser), and second, the dynamics of a (dynamically) injected semiconductor laser (the response laser).

An interpretation of the LFF phenomenon was given by Sano [17] in the framework of chaotic dynamics based on the LK model. He showed that the intensity dropouts correspond to crises between local attractors (Hopf unstable modes) and saddle-type antimodes. The dynamics of the system in the phase space shows a chaotic itinerancy with a drift towards a maximum gain mode (MGM) [15]. The trajectory is shown schematically in Fig. 3 (compare labels $1 \rightarrow 4$ in any of the loops to those in the inset time trace). The dynamics follows the path $1 \rightarrow 2 \rightarrow 3$ towards the MGM at region 3. The system jumps among the basins of attraction of the Hopf modes moving towards low frequencies. As the system evolves towards the MGM, the distance between modes and antimodes is reduced [17], and the probability that the trajectory falls into the

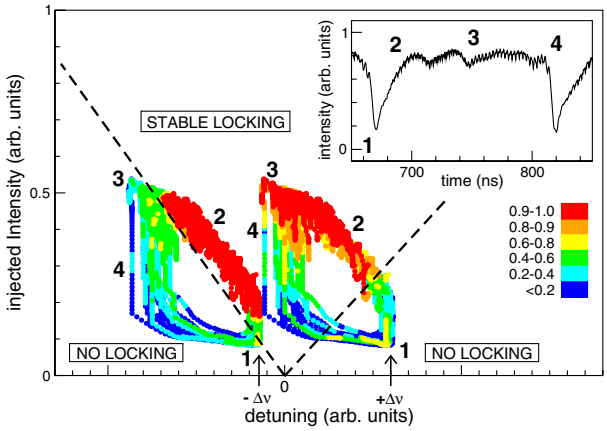

FIG. 3 (color online). Schematic illustration combining a qualitative sketch of the dynamical injection locking regime of the response laser [12] and a typical trajectory of the driving laser in the power-frequency plane for both positive and negative detuning. The arrows indicate the nominal detuning between the solitary emitter laser and the receiver laser. The inset shows the intensity time trace corresponding to the depicted trajectory. Color coding represents the sliding correlation coefficient (see text).

unstable manifold of an antimode increases. When the latter happens, the intensity suddenly drops and the frequency increases (path $3 \rightarrow 4 \rightarrow 1$ in Fig. 3). The buildup process begins right away, with the laser heading towards region 3 via path $1 \rightarrow 2 \rightarrow 3$ again. We note that the system spends most of the time close to the MGM in region 3.

The complex dynamics described above is injected into the response laser. The dynamics of an injected laser has been deeply studied in the case of continuous-wave (cw) or periodic injection. It is known that a detuning between the two lasers leads to different dynamical regimes and that an injection locking regime exists for small enough frequency detuning and injection strengths. For high values of these parameters injection locking is lost, and unlocked or unstable states appear [8]. Recent studies have shown that the locking range for synchronization by chaotic injection is similar to that of cw injection [12].

To explain the asymmetry in the desynchronization processes for positive and negative detuning in our case (see Fig. 1), we must take into account that the LFF dynamics of the driving laser leads to a substantial dynamical shift in frequency. The maximum frequency shift $\Delta\nu$ with respect to the solitary laser frequency (i.e., the shift corresponding to the MGM) can be estimated as $\Delta\nu = \alpha\kappa_f/2\pi$. As an example, for typical values of $\kappa_f = 0.025$ ps^{-1} and $\alpha = 3$ we obtain a frequency shift of $\Delta\nu \approx 12$ GHz. This frequency detuning lies within the injection locking regime of the response laser [12] for the coupling levels used in this Letter, which would guarantee full locking if the driving laser were at stable emission. Nevertheless, the driving laser does not have a stable output and its frequency, which as explained above changes in time, can leave the injection locking regime. In Fig. 3 we have outlined how the dy-

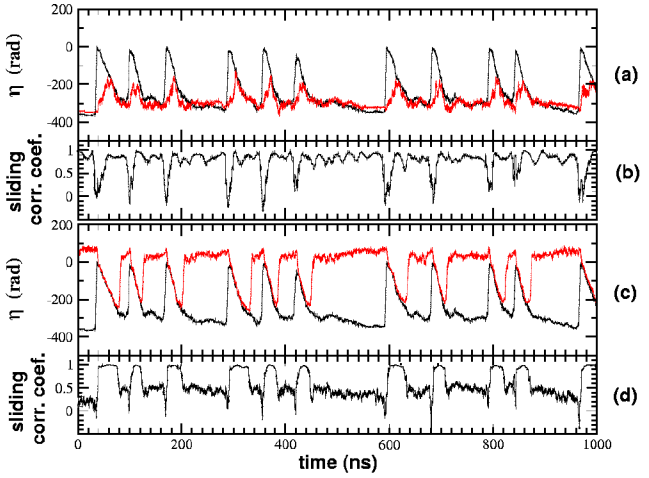

FIG. 4 (color online). Phase difference η accumulated during τ_f (a),(c) and time-dependent correlation coefficient (b),(d) for positive (a),(b) and negative (c),(d) detuning. In (a),(c) the black line represents the driving laser, and the gray (red) one the response laser.

namic injection from the driving laser leaves and reenters the locking regime. In this figure, the dynamical injection locking range is depicted only schematically; the accurate range has been numerically determined in Ref. [12] under similar conditions to our case. For moderate positive detuning (right trajectory), the dynamic injection spends most of the time within the locking region, leaving it only when the dropout takes place (at region 1). Consequently, the two lasers are synchronized most of the time, except when the driving laser undergoes a dropout. At that time synchronization is lost during a short transient, to be recovered again during buildup (beyond region 2). This leads to the behavior shown in Figs. 1(a) and 1(d).

In order to quantify the correlation between the lasers, we have computed the sliding (time-dependent) correlation coefficient between the intensity time series of driving and response lasers, defined as the value of the correlation function [12] at zero time difference, with temporal averages computed over a moving time window of width 3 ns. The result for positive detuning is shown in Fig. 4(b), together with the phase difference η after a time τ_f [Fig. 4(a)], which is related to the frequency drift. The plots show that the two lasers are strongly correlated most of the time, except when the driving laser [black line in 4(a)] undergoes a dropout, which the response laser is not able to follow. This is also seen in the color coding of Fig. 3, which plots the sliding correlation coefficient superimposed with the phase-space trajectory during dropouts.

When the detuning is negative (left trajectory in Fig. 3), the driving laser is outside the locking region of the response laser most of the time (i.e., at region 3), entering it only when a dropout occurs (after region 1). At that point, both lasers can synchronize, but as the driving laser recovers and gets back closer to the MGM (back to region 3), it leaves the locking region again and synchronization is lost. The result is that the two lasers are desynchronized most of the time, with brief synchronization episodes arising right after the dropouts in the emitter. This is the behavior shown in Figs. 1(c) and 1(f). Figures 4(c) and 4(d) show the frequency drift and sliding correlation coefficient between the two lasers for negative detuning. The synchronization episodes are clearly visible as short-lasting plateaus of correlation ~ 1 surrounded by long intervals of negligible correlation, corresponding to the times at which the driving laser is near its MGM.

In summary, we have shown that dynamic injection of a chaotic laser into a stable one leads to spontaneous episodes of synchronization for negative frequency detunings. This *episodic synchronization* can be expected to be a prevailing mechanism towards synchronization in systems with chaotic frequency cycles, and more generally in situations where the output of a broadband oscillator is injected into a second oscillator with a narrower locking range.

J. G. O. thanks A. Hutt and M. Zaks for discussions about the generality of episodic synchronization. Financial support was provided by MCyT-FEDER (Spain, Projects No. BFM2002-04369 and No. BFM2003-07850), and from the Generalitat de Catalunya.

*Present address: Department of Applied Physics and Photonics, Vrije Universiteit Brussel, Pleinlaan 2, B-1050 Brussels, Belgium.

[1] C. Schäfer *et al.*, Nature (London) **392**, 239 (1998).
[2] G. Vanwiggeren and R. Roy, Science **279**, 1198 (1998).
[3] A. Pikovsky, M. Rosenblum, and J. Kurths, *Synchronization* (Cambridge University Press, Cambridge, 2001).
[4] S. Boccaletti *et al.*, Phys. Rep. **366**, 1 (2002).
[5] W. J. Freeman and L. J. Rogers, J. Neurophysiol. **87**, 937 (2002).
[6] A. Hutt and H. Riedel, Physica (Amsterdam) **177D**, 203 (2003).
[7] E. Rodriguez *et al.*, Nature (London) **397**, 430 (1999).
[8] S. Wieczorek *et al.*, Phys. Rev. E **65**, 045207(R) (2002).
[9] Y. Takiguchi *et al.*, Opt. Lett. **24**, 1570 (1999).
[10] J. Revuelta *et al.*, IEEE Photonics Technol. Lett. **14**, 140 (2002).
[11] Y. Liu *et al.*, Appl. Phys. Lett. **80**, 4306 (2002).
[12] K. Kusumoto and J. Ohtsubo, IEEE J. Quantum Electron. **39**, 1531 (2003).
[13] A. Murakami, IEEE J. Quantum Electron. **39**, 438 (2003).
[14] I. V. Koryukin and P. Mandel, Phys. Rev. E **65**, 026201 (2002).
[15] I. Fischer *et al.*, Phys. Rev. Lett. **76**, 220 (1996).
[16] I. Wedekind and U. Parlitz, Phys. Rev. E **66**, 026218 (2002); S. Sivaprakasam *et al.*, Phys. Rev. A **64**, 013805 (2001).
[17] T. Sano, Phys. Rev. A **50**, 2719 (1994).